Published in final edited form as:

Biochim Biophys Acta. 2018 June ; 1863(6): 576–583. doi:10.1016/j.bbalip.2018.02.008.

Acetic acid induces Sch9-dependent translocation of Isc1p from the endoplasmic reticulum into mitochondria

António Rego[1,4], **Katrina F. Cooper**[2], **Justin Snider**[3], **Yusuf A. Hannun**[3], **Vítor Costa**[4,5,6], **Manuela Côrte-Real**[1,*], and **Susana Rodrigues Chaves**[1]

[1]Departamento de Biologia, Centro de Biologia Molecular e Ambiental, Universidade do Minho, Braga, Portugal

[2]Department of Molecular Biology, Graduate School of Biological Sciences, Rowan University, Stratford, NJ, 08084, USA

[3]Stony Brook Cancer Center, Stony Brook University, Health Science Center, Stony Brook, NY, USA

[4]Instituto de Investigação e Inovação em Saúde, Universidade do Porto, Porto, Portugal

[5]Instituto de Biologia Molecular e Celular, Universidade do Porto, Porto, Portugal

[6]Departamento de Biologia Molecular, Instituto de Ciências Biomédicas Abel Salazar, Universidade do Porto, Porto, Portugal

Abstract

Changes in sphingolipid metabolism have been linked to modulation of cell fate in both yeast and mammalian cells. We previously assessed the role of sphingolipids in cell death regulation using a well characterized yeast model of acetic acid-induced regulated cell death, finding that Isc1p, inositol phosphosphingolipid phospholipase C, plays a pro-death role in this process. Indeed, *isc1*Δ mutants exhibited a higher resistance to acetic acid associated with reduced mitochondrial alterations. Here, we show that Isc1p is regulated by Sch9p under acetic acid stress, since both single and double mutants lacking Isc1p or/and Sch9p have the same resistant phenotype, and *SCH9* deletion leads to a higher retention of Isc1p in the endoplasmic reticulum upon acetic acid exposure. We also found that the higher resistance of all mutants correlates with higher levels of endogenous mitochondrial phosphorylated long chain bases (LCBPs), suggesting that changing the sphingolipid balance in favour of LCBPs in mitochondria results in increased survival to acetic acid. In conclusion, our results suggest that Sch9p pathways modulate acetic acid-induced cell death, through the regulation of Isc1p cellular distribution, thus affecting the sphingolipid balance that regulates cell fate.

[*]Corresponding author: Manuela Côrte-Real, Universidade do Minho, Departamento de Biologia, Campus de Gualtar, 4710-057 Braga, Portugal. mcortereal@bio.uminho.pt.

Competing interests

No competing interests declared.

Keywords

Yeast; Cell signaling; Sphingolipids; Cell death; Acetic acid

1. Introduction

Sphingolipids are lipid second messengers generated in response to different physiological signals and stress stimuli. Alterations in the relative amounts of sphingolipids, particularly ceramide species, other intermediate metabolites such as long-chain bases (LCBs) and LCB-1-phosphates, and complex sphingolipid species, have significant effects on cell fate, mostly due to the effects of these molecules in both extrinsic and intrinsic pathways of apoptosis, in the activation of downstream effectors (protein kinases and phosphatases), modulation of protein trafficking, and activation of a variety of other signalling pathways [1]. Therefore, understanding how signaling pathways that regulate sphingolipid metabolism impact cell fate decisions will provide new clues to elucidating the underlying pathobiology of related human disorders, including cancer, autoimmune diseases and neurodegenerative disorders [2].

We have previously shown that the yeast *S. cerevisiae* provides an excellent model system to study how sphingolipid metabolism affects cell fate [3]. Indeed, studying regulated acetic acid-induced cell death that is dependent upon functional mitochondria, we uncovered a prominent role for Isc1p, the yeast inositol phosphosphingolipid phospholipase C. Isc1p, an orthologue of mammalian neutral sphingomyelinases-2, produces ceramides from complex sphingolipids and is required for normal mitochondrial function [4]. It has been implicated in the modulation of cellular responses to osmostress, heat stress, genotoxic agents, oxidative stress, and aging. Consistent with this, we showed that *isc1*Δ mutants exhibited a higher resistance to acetic acid that was associated with lower levels of ROS accumulation and reduced mitochondrial alterations, such as mitochondrial fragmentation and degradation, and decreased translocation of cytochrome *c* into the cytosol in response to acetic acid. We further showed that initial uptake rates and intracellular accumulation using ^{14}C-labelled acid in *isc1*Δ cells were not decreased when compared with their wild-type counterpart [3], discarding the possibility that changes in sphingolipid plasma membrane composition could alter the resistance of *S. cerevisiae isc1*Δ cells to acetic acid-induced cell death, as shown recently in *Zygosaccharomyces bailii* [5]. In contrast, *isc1Δ* cells showed decreased cellular levels of some ceramide species. This led us to conclude that acetic acid stress increases ceramide levels through hydrolysis of complex lipids by Isc1p, resulting in mitochondria-mediated regulated cell death (RCD) [3]. However, the signalling pathways involved in the activation of sphingolipid metabolism enzymes in this process remain poorly understood.

A recent study showed that the serine-threonine protein kinase Sch9p, the yeast orthologue of mammalian Akt and S6K proteins, is a major gatekeeper of sphingolipid homeostasis, functioning in a feedback system balancing ceramide production in response to both nutrient availability and sphingolipid signals [6]. Furthermore, it was shown in that study that Sch9p is required for efficient translocation of Isc1p from the endoplasmic reticulum (ER) to mitochondria during the diauxic shift. The authors postulated that this impaired translocation

of Isc1p in *sch9*Δ cells might abrogate the production of a specific mitochondrial pro-death ceramide pool, and hence lead to the long-lived phenotype of the *sch9*Δ strain [6]. Deletion of *SCH9* also increases resistance to acetic acid-induced death, which is consistent with the idea that the extension of chronological lifespan in *sch9*Δ mutants results from increased resistance to acetic acid produced during fermentation [7, 8]. The present work therefore aimed to unravel the role of the Sch9p kinase in acetic acid-induced cell death and its connection with Isc1p.

2. Materials and methods

2.1. Yeast strains, plasmids and growth conditions

The yeast *S. cerevisiae* BY4741 strain was used throughout this study as the wild-type. The wild-type and *sch9*Δ mutant strains were obtained from Euroscarf and *isc1*Δ and the double *isc1*Δ*sch9*Δ from [9]. Wild-type and *sch9*Δ cells were transformed with pYES2-*ISC1*-GFP [10] and pYX223-mitoCFP [11] by the LiAc method [12]. The mutants were selected on Synthetic Complete Glucose medium (SC Glu; 2% (w/v) Glucose, 0.67% (w/v) Yeast nitrogen base without aminoacids, 0.14% (w/v) Drop-out mixture lacking histidine, leucine, tryptophan and uracil, 0.008% (w/v) Histidine, 0.04% (w/v) Leucine, 0.008% (w/v) Tryptophan and 0.008% (w/v) Uracil) lacking the appropriate aminoacids.

2.2. Cell death assays

Strains were grown in SC Gal medium to early exponential phase (OD_{600} = 0.4–0.6) at 26° C in an orbital shaker at 200 rpm, with a ratio of flask volume/medium of 5:1. Strains transformed with plasmids were grown in the same medium lacking the appropriate aminoacids. For acetic acid treatment, the cultures were harvested and suspended in SC Gal medium at pH 3.0 (set with HCl) containing 140 mM of acetic acid (Panreac, Spain) for up to 180 min. Cell viability was measured as a percentage of colony forming units (c.f.u.) on YPD medium in relation to time 0.

2.3. Determination of plasma membrane integrity

Plasma membrane integrity was assessed by flow cytometry using Propidium Iodide (PI, Sigma-Aldrich) staining. PI was added to yeast cell suspensions to a final concentration of 5 μg/mL and incubated for 10 min at room temperature. Cells with red fluorescence [FL-3 channel (488/620 nm)] were considered to exhibit compromised plasma membrane integrity.

2.4. Superoxide anion accumulation assay

Intracellular superoxide anion was detected by flow cytometry using Dihydroethidium (DHE, Molecular Probes, Eugene, U.S.A.). Untreated or acetic acid-treated cells were harvested by centrifugation, suspended in PBS (80 mM Na_2HPO_4, 20 mM NaH_2PO_4 and 100 mM NaCl) and incubated in the dark with 5 μg/mL DHE for 30 min. Cells with red fluorescence [FL-3 channel (488/620 nm)] were considered to accumulate superoxide anion.

2.5. Flow cytometry assays

All flow cytometric assays were performed in an Epics® XLTM (Beckman Coulter) flow cytometer, equipped with an argon-ion laser emitting a 488-nm beam at 15 mW. The population of cells with high homogeneity and frequency was gated in a histogram of Side Scatter (SS) × Forward Scatter (FS). Twenty thousand cells per sample were analyzed. The resulting data were analyzed with WinMDI 2.8 software.

2.6. Determination of Isc1p localization

Untreated and acetic acid-treated cells transformed with pYES2-*ISC1*-GFP and pYX223-mitoCFP were observed by fluorescence microscopy. The images were obtained using a Nikon (Cedar Knolls, NJ) microscope (model E800) with a 100× objective (Plan Fluor Oil, numerical aperture 1.2) and a charge-coupled device camera (model C4742; Hamamatsu). Data were collected using NIS software and processed using Image Pro software. All images of individual cells were optically sectioned (0.2-μm slices at 0.6-μm spacing) and deconvolved, and the slices were collapsed to visualize the entire fluorescence signal within the cell.

2.7. Purified mitochondrial fractions and sphingolipid profiling

Purified mitochondrial fractions of untreated and acetic acid-treated cells were prepared as previously described [13]. Briefly, 1 L of cells were grown and treated under the same conditions as described above, harvested, washed and suspended in DTT Buffer (100 mM Tris/H2SO4 (pH 9.4), 10 mM Dithiothreitol). Cells were then digested with Zymolyase 100T (ImmunO, MP Biomedicals) to obtain spheroplasts and suspended in Homogenization buffer (10 mM Tris/HCl (pH 7.4), 0.6 M sorbitol, 1 mM EDTA, 0.2% (w/v) BSA). Spheroplasts were lysed with a few strokes in a glass Dounce homogenizer (tight fitting piston). Homogenates were centrifuged at 2500 rpm for 5 min and the supernatant then centrifuged at 12000 rpm for 15 min. To obtain pure mitochondria, free of contamination by other organelles, the pellet (crude mitochondrial fraction) was then subjected to further fractionation in a sucrose gradient (60% – 32% – 23% and 15% (w/v) sucrose). The crude mitochondrial fraction was placed on top of 15% (w/v) sucrose and centrifuged for 1 h at 33000 rpm at 4°C. The pure mitochondria was collected at the 60% – 32% sucrose interface and centrifuged for 30 min at 10000 g for 30 minutes at 4°C. The purity of ER-free mitochondrial fractions was confirmed by western blot using the primary antibody mouse monoclonal anti-HDEL (1:2000, Rockland), which detects Erd2p, a yeast ER lumen protein-retaining receptor (not shown). Lipids were extracted with a mixture of Ethyl acetate:iso-propanol:water at 60:30:10 (v/v/v/) [14]. The samples were resuspended in 150 μL mobile phase (Methanol, 1 mM Ammonium acetate and 0.2% (v/v) Formic acid). MS analyses were conducted on a TSQ Quantum Ultra triple quadrupole mass spectrometer with an Accela 1250 HPLC (Thermo Fisher Scientific, Waltham, MA, USA) for chromatographic separation. The lipids were separated on a Peek Scientific C-8 column (3 μm particle, 4.6 × 150 mm) at 45°C utilizing gradient conditions established by Bielawski [14] for the analysis of sphingolipid species. Mobile phase A was MS grade water containing 0.2% formic acid and 1 mM Ammonium formate (pH 5.6), and mobile phase B was MS grade Methanol containing 0.2% Formic acid and 1 mM Ammonium formate (pH 5.6). Detection by mass

spectrometer was performed in positive ion mode utilizing multiple reaction monitoring mode using transitions described in [14]. The ESI source parameters were maintained at 400°C vaporizer temperature and 300°C capillary temperature with a spray voltage of 3500 V. Gasses were set at 5, 40, and 10 for ion sweep, sheath, and auxiliary gases, respectively.

2.8. Reproducibility and statistical analysis of the results

Results are represented by mean and standard deviation (SD) values of at least three independent experiments. Statistical analyses were carried out using GraphPad Prism Software v5.00 (GraphPad Software, California, USA), Two-way ANOVA and Bonferroni Test. P-values lower than 0.05 were assumed to represent a significant difference.

3. Results and Discussion

3.1. Sch9p regulates acetic acid-induced cell death via Isc1p

To decipher the connection between Sch9p and Isc1p in acetic acid-induced RCD, we investigated whether disruption of *SCH9* affects the viability of *isc1*Δ mutant cells in response to acetic acid. For that purpose, exponentially growing *isc1*Δ*sch9*Δ double mutant cells and the corresponding single mutants (*isc1*Δ and *sch9*Δ), as well as wild-type control cells, were exposed to 140 mM acetic acid, pH 3.0, for 180 min and characterized regarding acetic acid-induced cell death (Figure 1).

In agreement with results obtained in a different strain background [3], deletion of *ISC1* in the BY4741 strain also increased the resistance of yeast cells to acetic acid-induced cell death (Figure 1A). Compared to wild type cells, *sch9*Δ and the double mutant had the same resistant phenotype, suggesting that Sch9p and Isc1p act in the same pathway in cell death induction. As we showed previously for wild-type and *isc1*Δ cells [3], both *sch9*Δ and *isc1*Δ*sch9*Δ cells maintained plasma membrane integrity (Figure 1B, measured by propidium iodide (PI) staining), which is consistent with an apoptotic cell death mechanism. Similarly, assessment of ROS accumulation in cells labelled with DHE also showed that the *isc1*Δ and *isc1*Δ*sch9*Δ resistance phenotype was associated with lower levels of superoxide anion whereas *sch9*Δ cells exhibited levels of this ROS identical to the wild-type (Figure 1C). Taken together, these results suggest that the higher resistance to acetic acid stress imparted by Sch9p depletion is not due to decreased superoxide anion accumulation. This indicates that in the *sch9*Δ background, in contrast to *isc1*Δ but as observed in the highly acetic acid resistant mutant *aac1/2/3Δ* [15], the apoptotic signal that proceeds from the mitochondria must be impaired downstream of ROS accumulation.

3.2. Acetic acid induces translocation of Isc1p from the endoplasmic reticulum into mitochondria via Sch9p

Previous studies demonstrated that Isc1p translocates to mitochondria during the diauxic shift, to produce a subset of phytoceramides [4, 16], and that deletion of *SCH9* impairs mitochondrial translocation of Isc1p in post-diauxic shift cells [6]. Since we established here that Sch9p regulates acetic acid-induced cell death, likely via Isc1p, we hypothesized that acetic acid could also induce translocation of Isc1p from the ER to mitochondria in a Sch9p-dependent manner. To test this hypothesis, we examined the subcellular localization of Isc1p

before and after acetic acid stress. Wild-type and *sch9*Δ strains expressing Isc1p-GFP and mitoCFP (blue fluorescent mitochondrial-specific marker) were grown in galactose medium (to induce *ISC1-GFP* expression), treated with acetic acid and analysed using fluorescence microscopy. The results (Figure 2A and quantitated in 2B) show that, in untreated wild-type and *sch9*Δ cells, Isc1p-GFP localized almost exclusively in the ER, without any significant co-localization with mitochondria. After exposure to acetic acid for 60 min, about of 32% of wild-type cells exhibited Isc1p-GFP in both ER and mitochondria and about 32% exclusively in the mitochondria (MIT). After 120 min, Isc1p-GFP was localized in mitochondria in practically all cells, as shown by co-localization with the mitochondrial marker. In contrast, *sch9*Δ cells showed higher retention of ER Isc1p-GFP, with only 36% exhibiting Isc1p-GFP exclusively in the mitochondria at the 120 minute time point. This suggests that the Sch9p kinase plays a role in translocating Isc1p from the ER to the mitochondria following acetic acid stress.

Previous studies have shown a change in localization of Isc1p between ER and mitochondria observed in different phases of the cell cycle [17]. Those studies could not distinguish if this change reflected translocation of protein from ER to mitochondria, or if that was a result of expression of new protein that became targeted to mitochondria. The acute effects of acetic acid allowed us to conduct studies to determine if Isc1p-GFP is truly translocated from the ER into mitochondria under acetic acid-induced cell death conditions, or is derived from newly synthesized Isc1p that is directly targeted to mitochondria. For this purpose, wild type and *sch9Δ* cells were grown in galactose, washed, switched to glucose medium (represses *GAL1* driven *ISC1-GFP* expression), and treated with acetic acid to monitor changes in Isc1p-GFP subcellular localization. As seen in Figure 3, Isc1p-GFP was still translocated and co-localized with mitochondria in wild-type cells exposed to acetic acid in glucose medium. At 30 min, Isc1p-GFP begun to translocate to mitochondria and after 60 min almost all cells already exhibited Isc1p-GFP exclusively in mitochondria. In *sch9*Δ cells, we also observed a higher retention of Isc1p-GFP in the ER. Indeed, at 120 min, only 39% of these cells exhibited Isc1p-GFP in mitochondria. These results show that deletion of *SCH9* impairs mitochondrial translocation of Isc1p in response to acetic acid independently of the carbon source used, and that translocation does not require *de novo* Isc1p synthesis.

Since deletion of *SCH9* does not prevent ROS accumulation in response to acetic acid, the above results support the model that Sch9p-mediated mitochondrial localization of Isc1p is required for efficient acetic acid-induced RCD independently or downstream of ROS accumulation. Indeed, as the *isc1*Δ *sch9*Δ double mutant exhibits a similar phenotype as the *isc1*Δ single mutant, which does not display decreased acetic acid uptake [3], it is unlikely that the resistance phenotype is due to altered sphingolipid concentration in the plasma membrane and would be upstream to an intracellular regulator mechanism. Some studies demonstrated that Isc1p has a role in the Sch9p-dependent phenotypes [18–20]. However, loss of Sch9p results in increased resistance to oxidative stress and extension of chronological lifespan [8, 21], whereas loss of Isc1p can be associated with both pro-survival and pro-death roles. For instance, Isc1p depletion can confer higher oxidative stress sensitivity and reduced chronological lifespan [18] or acetic acid resistance [3], respectively. Impaired translocation of Isc1p into mitochondria may contribute in part to the increased longevity observed in the *sch9*Δ strain, due to the reduction of mitochondrial ceramide

species and consequently decreased mitochondrial membrane permeabilization. However, the pro-death function of Isc1p does not correlate with the higher sensitivity of cells lacking *ISC1* to hydrogen peroxide. On the other hand, the higher resistance of the *isc1*Δ mutant and the Isc1p translocation into mitochondria during acetic acid-induced cell death suggest that acetic acid prompts, possibly via Sch9p, Isc1p-dependent generation of pro-death ceramides in mitochondria.

3.3. The resistance of isc1Δ, sch9Δ and isc1Δsch9Δ mutants to acetic acid is associated with increased levels of LCB-1-P in mitochondria

The above results suggest a model in which, following acetic acid exposure, Isc1p moves to the mitochondria, where it is required to hydrolyse mitochondrial sphingolipids into the pro-death ceramide species. This model is consistent with the idea that the increased lifespan observed in *isc1Δ* and *sch9Δ* cells is due to a build-up of mitochondrial sphingolipids. To test this hypothesis, we performed a mitochondrial lipidomic analysis of wild type, *isc1*Δ, *sch9*Δ and *isc1*Δ*sch9*Δ cells in response to acetic acid. Even though survival levels were only statistically significant at the 180 min time point, since it is after 120 min of acetic acid treatment that the differences in translocation of Isc1p-GFP are evident, we isolated mitochondria before and after 120 min of exposure for further analysis of the levels of bioactive sphingolipid species: LCBs (dihydrosphingosine (DHS), phytosphingosine (PHS), their phosphorylated counterparts DHS-1-P and PHS-1-P), and ceramides [dihydroceramides (DhCer), phytoceramides (PhytoCer) and α-hydroxylated-phytoceramides (α-OH-PhytoCer)] (Figure 4A).

Analysis of the relative basal levels of bioactive sphingolipid species of the mutants in relation to wild-type cells did not reveal many similarities. Indeed, several sphingolipid species decreased, some were not affected, and others increased differently with deletion of *ISC1* and/or *SCH9* (Figure 4B). For instance, *ISC1* deletion increased basal levels of PHS, DHS and DhCer, whereas deletion of *SCH9* decreased basal levels of PHS, PHS-1-P and DHS-1-P. On the other hand, deletion of both *ISC1* and *SCH9* increased basal levels of almost all sphingolipids in comparison with wild-type cells, namely PHS, DHS, PHS-1-P, DHS-1-P, PhytoCer and DhCer. However, *isc1*Δ, *sch9*Δ and *isc1*Δ*sch9*Δ mutants did display one common pattern, with significant lower basal levels of α-OH-PhytoCer, which may contribute to the higher resistance of these mutants to acetic acid. This indicates that Sch9p and Isc1p can play both different and overlapping roles in sphingolipid metabolism.

After exposure of wild-type cells to acetic acid, the most notable changes were significant decreases in PHS-1-P and DHS-1-P, as well as of α-OH-PhytoCer, and an increase in DHCer levels. Unexpectedly, all mutants displayed similar or higher absolute levels of all sphingolipids in mitochondria than the wild-type strain, with the exception of α-OH-PhytoCer (Figure 4A). Nonetheless, further analyzing the ratio between absolute levels of sphingolipids after 120 min exposure in relation to time 0 revealed interesting differences between the wild-type strain and the resistant mutants (Figure 4C), as discussed below.

In our previous lipidomic analysis of whole cells, we observed that acetic acid induced an increase of PhytoCer species in wild-type and not in *isc1*Δ cells, leading us to postulate that acetic acid induces cell death through production of phytoceramides via Isc1p [3]. In

contrast, in lipidomic analysis of mitochondria we now observe an increase of PhytoCer in *isc1*Δ as well as in *sch9*Δ and *isc1*Δ*sch9*Δ mutants. A previous study suggested that DhCer may be detrimental in the acetic acid response [22]. However, our results show that DhCer increased in mitochondria of all the strains, including in wild-type. The analysis of the different DhCer and PhytoCer species did not reveal any particular species that increased in wild-type but not in the mutant cells, ruling out the hypothesis that some of these species might mediate the toxicity in acetic acid-induced cell death. We also considered the possibility that one of the DhCer or PhytoCer species could have protective effects. In that case, its levels should be higher in the mutants (either basally or after acetic acid). Interestingly, we found multiple species whose levels were higher in the mutant strains only after acetic acid treatment, namely $DhC_{18:1}$-Cer, DhC_{22}-Cer, $PhytoC_{18}$-Cer and $PhytoC_{28}$-Cer, or both basally and after acetic acid treatment, namely $DhC_{20:1}$-Cer, DhC_{20}-Cer, $PhytoC_{22}$-Cer, $PhytoC_{24}$-Cer and $PhytoC_{26}$-Cer. Regarding the increased levels of DhCer species, it might be important in the inhibition of the assembly of ceramide channels in mitochondria, as postulated by [23], and consequently in the higher resistance of *isc1*Δ, *sch9*Δ and *isc1*Δ*sch9*Δ mutants to acetic acid. However, the involvement of these sphingolipids species in acetic acid-induced cell death seems complex.

We also observed that, though the levels of α-OH-PhytoCer decreased in wild-type cells but increased in all the other mutants upon exposure to acetic acid, absolute levels did not surpass those observed in wild-type cells, which is still consistent with the hypothesis that lower levels of α-OH-PhytoCer may contribute to the higher resistance of *isc1*Δ, *sch9*Δ and *isc1*Δ*sch9*Δ mutants.

On the other hand, analysis of the levels of both DHS-1-P and/or PHS-1-P, associated with a pro-survival role, also revealed that these sphingolipid species decreased in mitochondria of wild-type cell but increased in *isc1*Δ, *sch9*Δ and *isc1*Δ*sch9*Δ mutants, which suggests that elevation in LCBPs may contribute to the increased survival of the mutants exposed to acetic acid. Interestingly, several other studies also have suggested LCBPs are involved in increased survival to heat-stress in yeast [24], and in mammalian cells [25, 26]. Therefore, it seems that the dynamic balance between phytoceramides and phosphorylated LCBs is important to determine cell fate upon acetic acid-induced cell death, but our results suggest that it is changing the sphingolipid balance in favour of the LCBPs in mitochondria and whole cells that result in increased survival to acetic acid.

4. Conclusions

In this study, we gained several important new insights into the regulation of cell fate through sphingolipid metabolism in the well-characterized acetic-acid induced yeast cell death system. We demonstrate for the first time that a stress stimulus can induce Sch9p-dependent translocation of Isc1p from the endoplasmic reticulum to mitochondria. Moreover, while the balance between phytoceramides and phosphorylated LCBs determines cell fate, we found that disruption of the Sch9p/Isc1p pathway results in increased survival to acetic acid likely due to accumulation of LCBPs in mitochondria, through a yet uncharacterized mechanism. One possibility is that deletion of Isc1p and/or Sch9p affects the expression and activity of biosynthesis/breakdown enzymes in production of LCBPs

(and ceramides) during acetic acid-induced cell death, though we cannot exclude the involvement of mechanisms that affect the transcriptional regulation of genes encoding ceramide synthases, ceramidases, or SPT activity, likely through phosphorylation of Orm proteins, or others.

Taken together, our results raise the hypothesis that LCBPs in general can tilt the scale towards survival in the intricate balance between sphingolipid-mediated life and death.

Acknowledgments

Funding

This project was financially supported by Fundação para a Ciência e Tecnologia (FCT) by means of a fellowship to A.R (SFRH/BD/79523/2011) and to S.R.C. (SFRH/BPD/89980/2012), and by projects Pest-C/BIA/UI4050/2011, FCOMP-01-0124-FEDER-027652, FCOMP-01-0124-FEDER-028210, Pest-C/SAU/LA0002/2011, FCOMP-01-0124-FEDER-022718, PTDC/BBB-BQB/1850/2012, FCT-ANR/BEXBCM/0175/2012, and UID/BIM/04293/2013. KFC and YAH are funded by National Institutes of Health Grant numbers GM113196 and GM118128, respectively.

References

1. Cowart LA, Obeid LM. Yeast sphingolipids: recent developments in understanding biosynthesis, regulation, and function. Biochim Biophys Acta. 2007; 1771:421–431. [PubMed: 16997623]
2. Fischer U, Schulze-Osthoff K. Apoptosis-based therapies and drug targets. Cell Death Differ. 2005; 12(Suppl 1):942–961. [PubMed: 15665817]
3. Rego A, Costa M, Chaves SR, Matmati N, Pereira H, Sousa MJ, Moradas-Ferreira P, Hannun YA, Costa V, Corte-Real M. Modulation of mitochondrial outer membrane permeabilization and apoptosis by ceramide metabolism. PLoS One. 2012; 7:e48571. [PubMed: 23226203]
4. Kitagaki H, Cowart LA, Matmati N, Vaena de Avalos S, Novgorodov SA, Zeidan YH, Bielawski J, Obeid LM, Hannun YA. Isc1 regulates sphingolipid metabolism in yeast mitochondria. Biochim Biophys Acta. 2007; 1768:2849–2861. [PubMed: 17880915]
5. Lindahl L, Genheden S, Eriksson LA, Olsson L, Bettiga M. Sphingolipids contribute to acetic acid resistance in Zygosaccharomyces bailii. Biotechnol Bioeng. 2016; 113:744–753. [PubMed: 26416641]
6. Swinnen E, Wilms T, Idkowiak-Baldys J, Smets B, De Snijder P, Accardo S, Ghillebert R, Thevissen K, Cammue B, De Vos D, Bielawski J, Hannun YA, Winderickx J. The protein kinase Sch9 is a key regulator of sphingolipid metabolism in Saccharomyces cerevisiae. Mol Biol Cell. 2014; 25:196–211. [PubMed: 24196832]
7. Burtner CR, Murakami CJ, Kennedy BK, Kaeberlein M. A molecular mechanism of chronological aging in yeast. Cell Cycle. 2009; 8:1256–1270. [PubMed: 19305133]
8. Huang X, Liu J, Dickson RC. Down-regulating sphingolipid synthesis increases yeast lifespan. PLoS Genet. 2012; 8:e1002493. [PubMed: 22319457]
9. Teixeira V, Medeiros TC, Vilaca R, Moradas-Ferreira P, Costa V. Reduced TORC1 signaling abolishes mitochondrial dysfunctions and shortened chronological lifespan of Isc1p-deficient cells. Microb Cell. 2014; 1:21–36. [PubMed: 28357207]
10. Sawai H, Okamoto Y, Luberto C, Mao C, Bielawska A, Domae N, Hannun YA. Identification of ISC1 (YER019w) as inositol phosphosphingolipid phospholipase C in Saccharomyces cerevisiae. J Biol Chem. 2000; 275:39793–39798. [PubMed: 11006294]
11. Naylor K, Ingerman E, Okreglak V, Marino M, Hinshaw JE, Nunnari J. Mdv1 interacts with assembled dnm1 to promote mitochondrial division. J Biol Chem. 2006; 281:2177–2183. [PubMed: 16272155]
12. Gietz RD, Woods RA. Transformation of yeast by lithium acetate/single-stranded carrier DNA/polyethylene glycol method. Methods Enzymol. 2002; 350:87–96. [PubMed: 12073338]
13. Gregg C, Kyryakov P, Titorenko VI. Purification of mitochondria from yeast cells. J Vis Exp. 2009

14. Bielawski J, Pierce JS, Snider J, Rembiesa B, Szulc ZM, Bielawska A. Comprehensive quantitative analysis of bioactive sphingolipids by high-performance liquid chromatography-tandem mass spectrometry. Methods Mol Biol. 2009; 579:443–467. [PubMed: 19763489]
15. Pereira C, Camougrand N, Manon S, Sousa MJ, Corte-Real M. ADP/ATP carrier is required for mitochondrial outer membrane permeabilization and cytochrome *c* release in yeast apoptosis. Mol Microbiol. 2007; 66:571–582. [PubMed: 17822411]
16. Vaena de Avalos S, Su X, Zhang M, Okamoto Y, Dowhan W, Hannun YA. The phosphatidylglycerol/cardiolipin biosynthetic pathway is required for the activation of inositol phosphosphingolipid phospholipase C, Isc1p, during growth of Saccharomyces cerevisiae. J Biol Chem. 2005; 280:7170–7177. [PubMed: 15611094]
17. Vaena de Avalos S, Okamoto Y, Hannun YA. Activation and localization of inositol phosphosphingolipid phospholipase C, Isc1p, to the mitochondria during growth of *Saccharomyces cerevisiae*. J Biol Chem. 2004; 279:11537–11545. [PubMed: 14699160]
18. Almeida T, Marques M, Mojzita D, Amorim MA, Silva RD, Almeida B, Rodrigues P, Ludovico P, Hohmann S, Moradas-Ferreira P, Corte-Real M, Costa V. Isc1p plays a key role in hydrogen peroxide resistance and chronological lifespan through modulation of iron levels and apoptosis. Mol Biol Cell. 2008; 19:865–876. [PubMed: 18162582]
19. Kitagaki H, Cowart LA, Matmati N, Montefusco D, Gandy J, de Avalos SV, Novgorodov SA, Zheng J, Obeid LM, Hannun YA. ISC1-dependent metabolic adaptation reveals an indispensable role for mitochondria in induction of nuclear genes during the diauxic shift in Saccharomyces cerevisiae. J Biol Chem. 2009; 284:10818–10830. [PubMed: 19179331]
20. Barbosa AD, Osorio H, Sims KJ, Almeida T, Alves M, Bielawski J, Amorim MA, Moradas-Ferreira P, Hannun YA, Costa V. Role for Sit4p-dependent mitochondrial dysfunction in mediating the shortened chronological lifespan and oxidative stress sensitivity of Isc1p-deficient cells. Mol Microbiol. 2011; 81:515–527. [PubMed: 21707788]
21. Fabrizio P, Pozza F, Pletcher SD, Gendron CM, Longo VD. Regulation of longevity and stress resistance by Sch9 in yeast. Science. 2001; 292:288–290. [PubMed: 11292860]
22. Montefusco DJ, Chen L, Matmati N, Lu S, Newcomb B, Cooper GF, Hannun YA, Lu X. Distinct signaling roles of ceramide species in yeast revealed through systematic perturbation and systems biology analyses. Sci Signal. 2013; 6:rs14. [PubMed: 24170935]
23. Stiban J, Fistere D, Colombini M. Dihydroceramide hinders ceramide channel formation: Implications on apoptosis. Apoptosis. 2006; 11:773–780. [PubMed: 16532372]
24. Skrzypek MS, Nagiec MM, Lester RL, Dickson RC. Analysis of phosphorylated sphingolipid long-chain bases reveals potential roles in heat stress and growth control in Saccharomyces. J Bacteriol. 1999; 181:1134–1140. [PubMed: 9973338]
25. Saddoughi SA, Song P, Ogretmen B. Roles of bioactive sphingolipids in cancer biology and therapeutics. Subcell Biochem. 2008; 49:413–440. [PubMed: 18751921]
26. Van Brocklyn JR, Williams JB. The control of the balance between ceramide and sphingosine-1-phosphate by sphingosine kinase: oxidative stress and the seesaw of cell survival and death. Comp Biochem Physiol B Biochem Mol Biol. 2012; 163:26–36. [PubMed: 22613819]

Highlights

- The Sch9p pathway modulates acetic acid-induced cell death
- Isc1p is regulated by Sch9p in cells under acetic acid stress
- *SCH9* deletion increases Isc1p retention in the ER in cells exposed to acetic acid
- The Isc1p cellular distribution affects sphingolipid balance and cell fate
- Favouring the increase of LCBPs in mitochondria increases survival to acetic acid

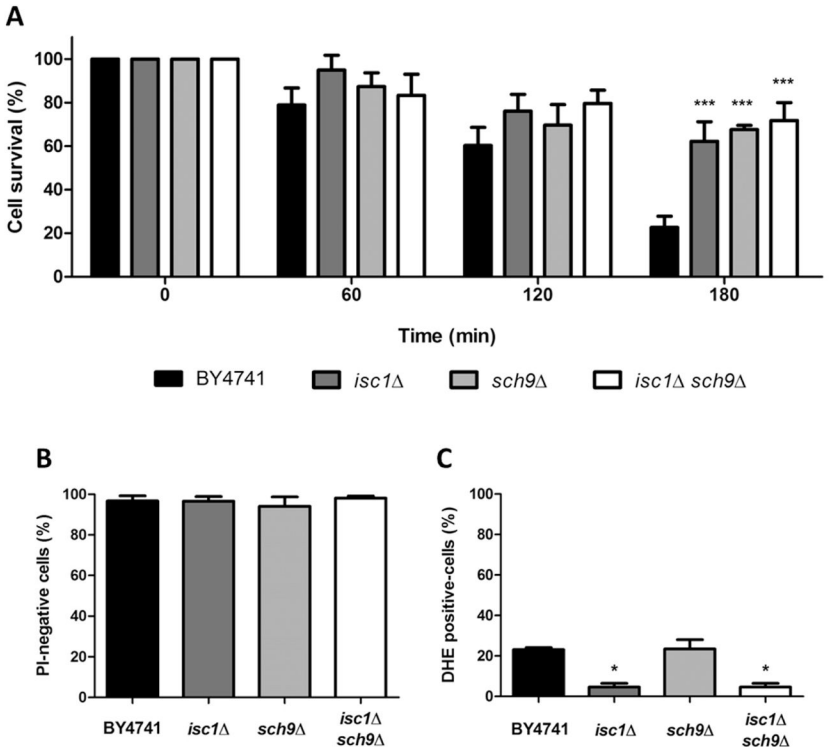

Figure 1. Sch9p regulates acetic acid-induced cell death

A) Cell survival of the indicated strains to 140 mM of acetic acid, pH 3.0, for 180 min. B) Percentage of PI-negative cells after acetic acid exposure. C) Levels of superoxide anion in the indicated strains exposed to acetic acid using DHE. Values significantly different from the BY4741 strain: * $P < 0.05$, *** $P < 0.001$.

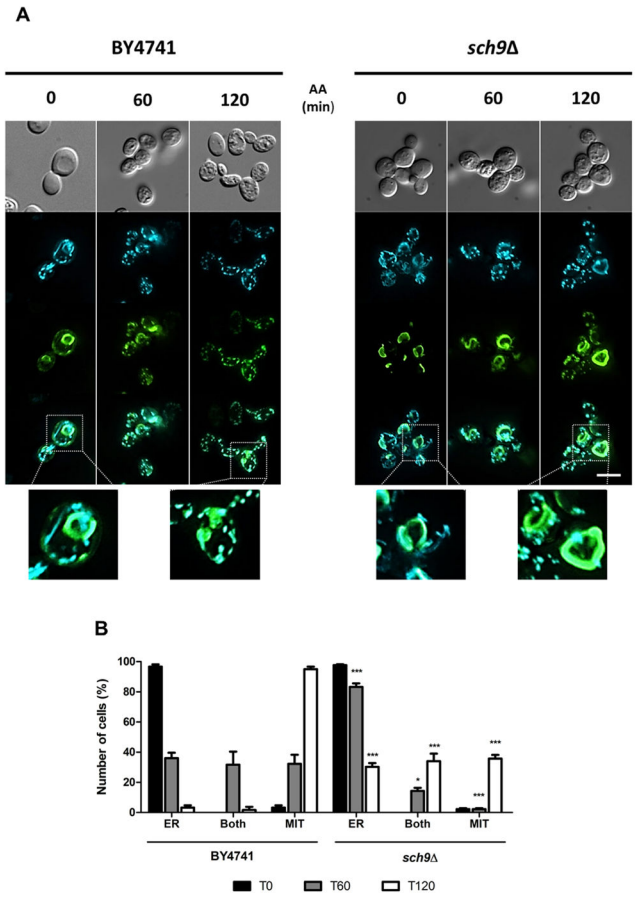

Figure 2. Translocation of Isc1p from ER into mitochondria in galactose-grown cells

A) Isc1p-GFP localization in the indicated strains grown and treated in SC galactose medium before and after exposure to 140 mM of acetic acid, pH 3.0, for up to 120 min. MitoCFP (blue) was used to label mitochondria. B) Quantification of the number of cells with Isc1p in the endoplasmic reticulum (ER), mitochondria (MIT) or both organelles (Both). Values significantly different from the BY4741 strain: * $P < 0.05$, *** $P < 0.001$. Bar, 5 μm.

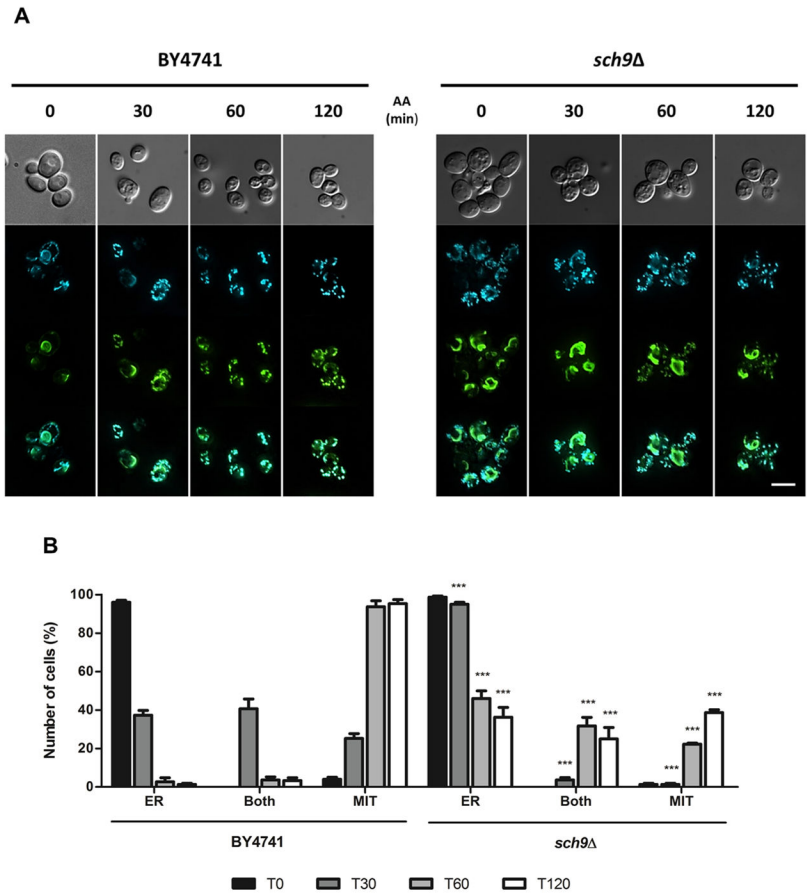

Figure 3. Translocation of Isc1p from ER into mitochondria in glucose-grown cells

A) Isc1p-GFP localization in the indicated strains grown in SC galactose medium, shifted into SC glucose medium and exposed to 140 mM of acetic acid, pH 3.0, for up to 120 min. Mt-CFP (blue) was used to stain mitochondria. B) Quantification of the number of cells with Isc1p in the endoplasmic reticulum (ER), mitochondria (MIT) or both organelles (BOTH). Values significantly different from the BY4741 strain: *** $P < 0.001$. Bar, 5 μm.

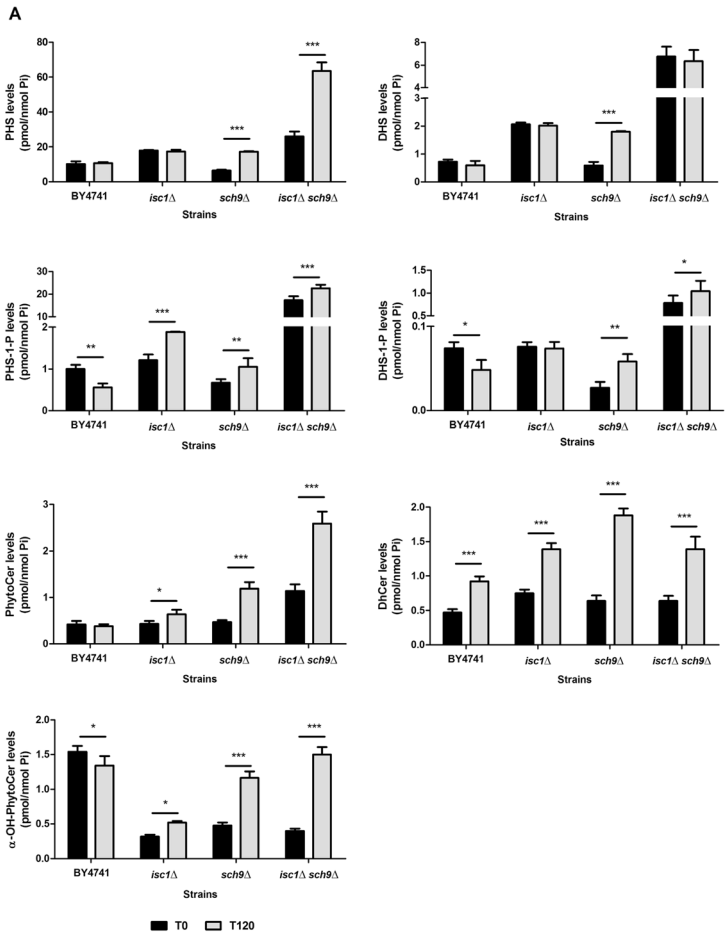

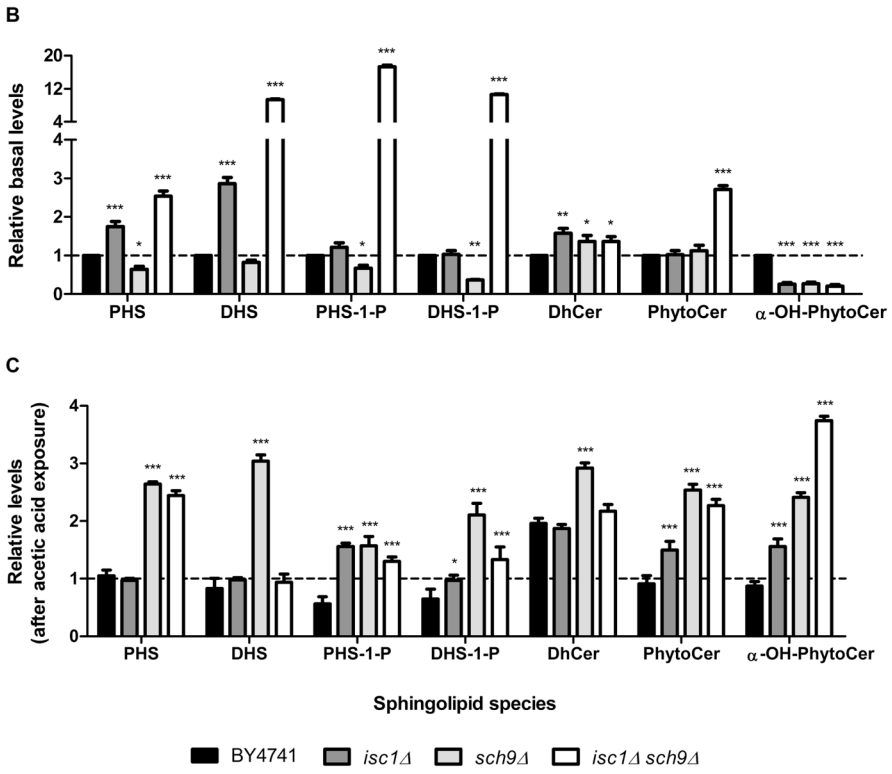

Figure 4. Levels of sphingolipid species in purified mitochondria before and after acetic acid exposure

Absolute levels (A) and relative levels (B and C) of dihydrosphingosine (DHS), dihydrosphingosine-1-phosphate (DHS-1P), dihydroceramide (dhCer), phytosphingosine (PHS), phytosphingosine-1-phosphate (PHS-1P), phytoceramides (PhytoCer) and α-hydroxylated phytoceramide (OH-PhytoCer) in mitochondria from *S. cerevisiae* BY4741 (wild-type), *isc1*Δ, *sch9*Δ and *isc1*Δ *sch9*Δ strains before and after exposure to 140 mM acetic acid, pH 3.0, for 120 min are shown. * P<0.05, ** P<0.01, *** P < 0.001.